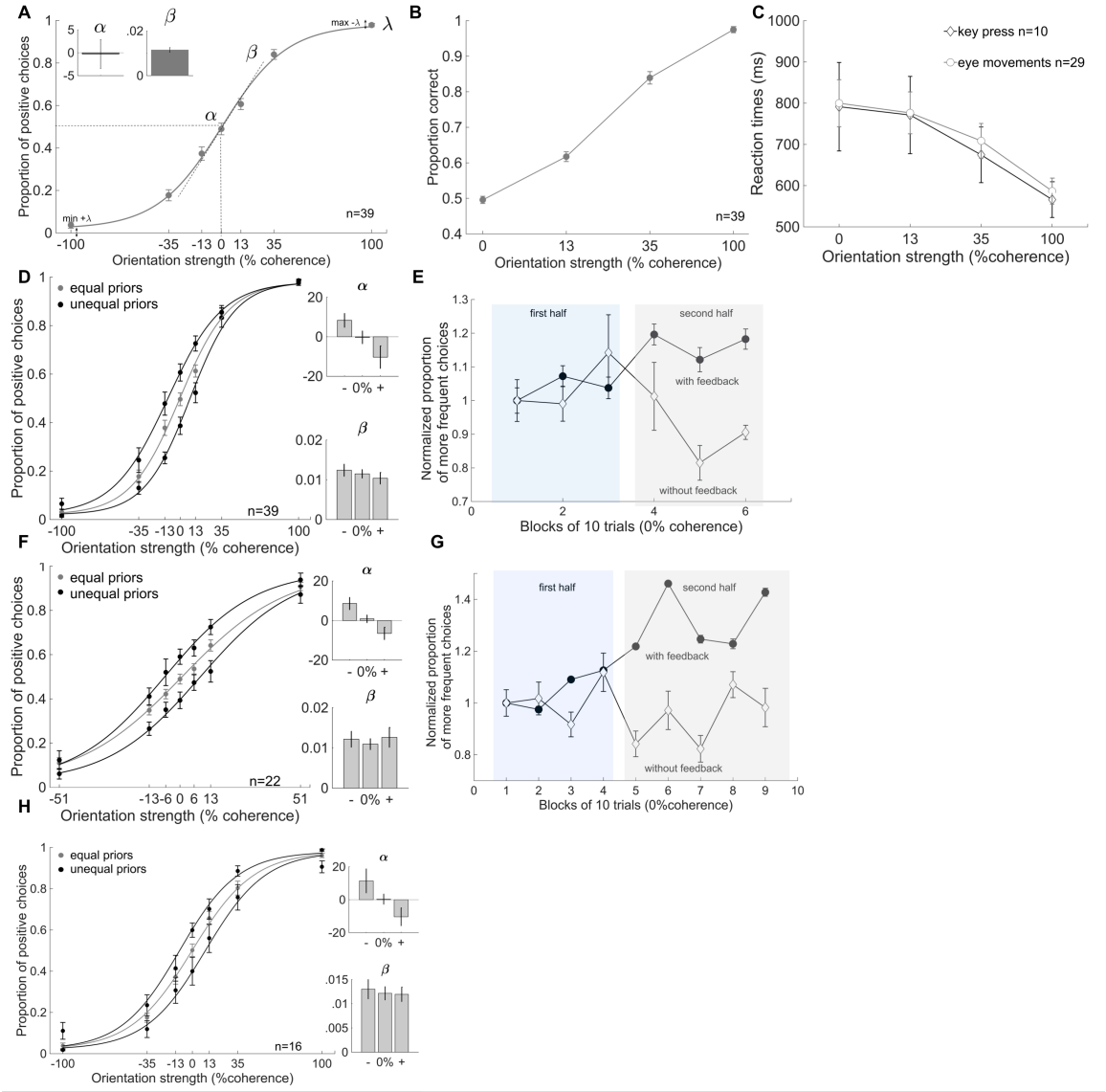

Figure S1. Validation of the tasks in young healthy participants. Related to Figure 1, Figure 3, and Figure 4.

(A-E) Dichromatic task (F-G) Monochromatic task (H) Explicit task

(A) Proportion of positive choices (leftward choices) is plotted against orientation strength for a group of 39 young healthy participants (yHC). These data are fitted with a logistic function of the form, $p(P) = \lambda + (1-2*\lambda)/(1+\exp(-\beta (C-\alpha)))$; where $p(P)$ is the proportion of positive choices and C is dot pair coherence. α and β are free parameters determined using maximum likelihood methods, and provide a measure of the response bias (α) and the slope or sensitivity of the psychometric function (β). The lapse rate λ is the difference between the asymptote of the function and perfect performance. It is assumed to arise from transient lapses in attention during task performance. The parameters of the fits were used to compare performance between the equal and unequal prior conditions within groups. Insets show histograms of α and β parameters from the fitted function.

(B) Example performance of n = 39 yHC (mean age = 22.5yrs; 14 males and 25 females). The proportion of correct choices is plotted against the orientation strength. At 0% coherence there is no information about orientation and performance is ~50% correct, as expected. Participants accurately discriminated the orientation with 100% dot pair coherence regardless of the color of the stimulus, and their performance

increased as the strength of the sensory information increased (ANOVA, $F_{(3,155)}$=277.57, p<0.0001). Performance was at chance level for the stimulus containing only noise (0%).

(C) RT for the 39 yHC is plotted against dot pair coherence for the key press (diamonds) and eye movement responses (circles) separately. Consistent with models proposing that noisy sensory evidence is integrated over time to reach a decision, reaction times (RTs) were shorter for stimuli with higher coherence and significantly longer for lower coherence stimuli (ANOVA, $F_{(3,160)}$=6.56, p<0.0001) for both saccades and computer key presses (ANOVA, $F_{(1,160)}$=0.69, p>0.05). The interaction between coherence level and response modality was not significant (ANOVA, $F_{(3,160)}$=0.004, p>0.05). Since the data for both the button press and the eye movement responses were similar, we pooled the data for this report for all figures except what is shown in this figure. Note that B and C taken together show that this behavior is well-suited for integration to threshold models of decision-making.

(D) Proportion of positive choices is plotted against orientation strength for the 39 yHC performing the task with trial-by-trial feedback. The grey points and lines show the data and the logistic fits in the equal prior trials (50:50) whereas the black points and lines show the data for unequal prior trials (75:25). The direction and color of the stimulus with different priors were counterbalanced across participants so that all participants contributed to the grey data and different subsets of participants contributed to the black data. yHC were able to incorporate the prior in their decisions in the dichromatic task, as shown by a shift in their response bias (α parameter of the logistic fit, see Insets).

(E) Proportion of choices in favor of the most frequent direction is plotted against the trial number in the 0% coherence condition for the group of participants performing the task with trial-by-trial feedback (black circles, 39yHC of (D)), and the group performing the dichromatic task without feedback (open circles, n = 6, 3 females, 3 males, mean age 20.2yrs). Data are normalized to the mean of the first 10 trials. The rate of learning in the group provided with trial-by-trial feedback is indicated by the positive slope of the linear regression calculated taking into account all data points from the first data point to the last data point (slope = 0.035, 95% CI [0.001, 0.067]) and shows that participants learned the bias gradually by the second half of the block (gray shading). With feedback, the influence of the priors appeared gradually and was most apparent during the second half of the trials (black circles, grey shading). Without feedback, participants failed to develop a bias as confirmed statistically by the negative slope of the linear regression (-0.03, 95% CI [-0.100, 0.036]) (open circles). Confirming this statistically, during the first half of the trials both groups performed similarly (cyan shaded area, $t(45)$= 1.01, p > 0.05) but performance between the groups showed a significant separation during the second half of the trials (gray shaded area, $t(45)$=14.07 p < 0.001). These results indicate that even though there is no explicit reward, feedback is required for healthy participants to learn the prior information in this task.

(F) Young healthy participants performing the monochromatic task. Proportion of positive choices is plotted against orientation strength for 22 yHC (14 females and 8 males, mean age 20yrs) performing the task with trial-by-trial feedback. Data are plotted as in (D). yHC were able to incorporate the prior in their decisions during the monochromatic task, as shown by a shift in their response bias (α parameter of the logistic fit, see Inset).

(G) Proportion of choices in favor of the most frequent orientation is plotted against the trial number in the 0% coherence condition for the group of 22 yHC that performed the task with feedback condition as in (E) (black circles) and the groups of 14 yHC performing the monochromatic task without feedback (11 females, 3 males, mean age 19.9yrs). With trial-by-trial feedback, participants gradually accumulate the prior over time as indicated by the positive slope of the linear regression from the first data point to the last data point of the unequal prior block (slope is 0.05, 95% CI [0.021, 0.082]). Without feedback, participants do not learn the prior over time as confirmed statistically by the slope of the linear regression from the first data point to the last data point of the unequal prior block (slope is 0.004, 95% CI [-0.035, 0.027]). During the first half of the trials (cyan shaded area) both with and without feedback groups performed similarly (cyan shaded area, $t(35)$=1.23, p>0.05) but they performed differently during the second half of the trials (grey shaded area, $t(35)$=5.69, p<0.0001). Based on this we conclude that although the direction of the prior is more obvious in the monochromatic task compared to the dichromatic task, feedback is still necessary for learning the priors.

(H) Young healthy participants performing the dichromatic task with explicit prior instructions but without trial-by-trial feedback. Proportion of positive choices is plotted against the orientation strength for 16 yHC (13 females, 3 males, mean age 20.1 yrs). As in Figure D, the grey points and line show the equal prior trials whereas the black points and lines show the unequal prior trials. yHC were able to incorporate the

prior in their decisions during the dichromatic task with explicit instructions, as shown by a shift in their response bias (α parameter of the logistic fit, see Inset).The insets show the parameters of the logistic fits. In all panels, error bars are ±SEM.

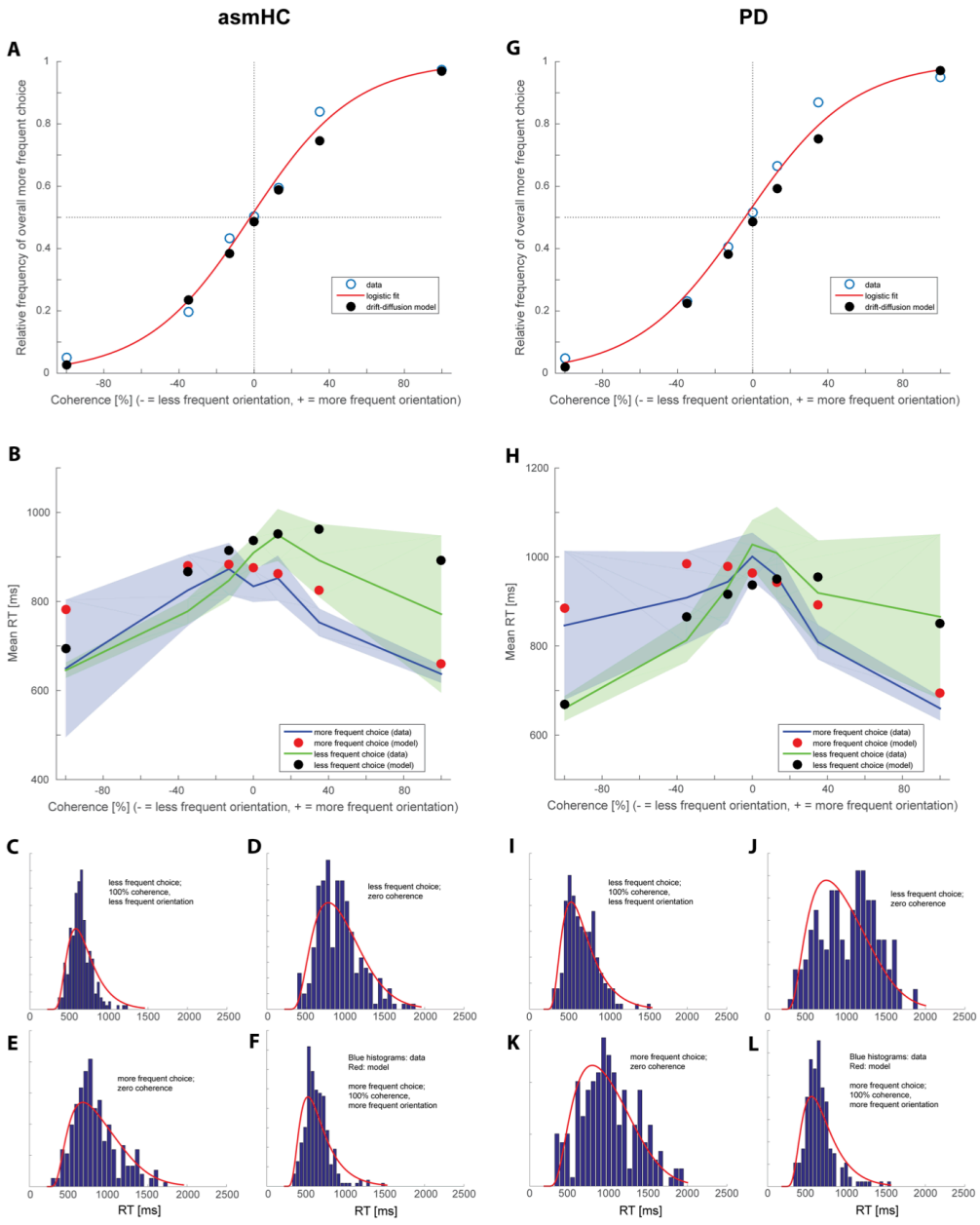

Figure S2. Model fits for choices and RTs for the dichromatic task. Related to Figure 2.
(A-F) asmHC participants, (G-L) Patients with Parkinson's disease (PD)
(A) Psychometric function showing the proportion of the "more frequent choice" as a function of stimulus coherence and orientation. Positive coherence values correspond to the orientation shown more frequently and negative values correspond to the less frequent orientation. Open circles are data, the red line is the maximum likelihood logistic fit, and filled circles are the model predictions.
(B) Mean RT is plotted as a function of stimulus coherence and orientation as in A. The blue line shows the mean RT for the "more frequent choice", the shaded area indicates the 95% confidence interval. The red symbols show the model predictions for the "more frequent choice". The green line shows the mean RT for the "less frequent choice" (the choice that, according to the priors, should be overall less frequent) and the shaded area again indicates the 95% confidence interval. The black symbols show the corresponding model predictions.

(C) RT distribution for the highest coherence and the less frequent orientation. Only correct choices (“less frequent choice”) are shown because errors are rare for the highest coherence, thus they do not have a well-defined RT distribution. Data are shown as blue histograms, the model predictions as red lines.
(D) RT distribution for zero coherence and the “less frequent choice”. Data are shown as blue histograms, the model predictions as red lines.
(E) Same as (D) but for the ”more frequent choice”.
(F) Same as (C) but for the more frequent orientation and the “more frequent choice”.
(G-L) Same as in (A-F), but for patients with PD

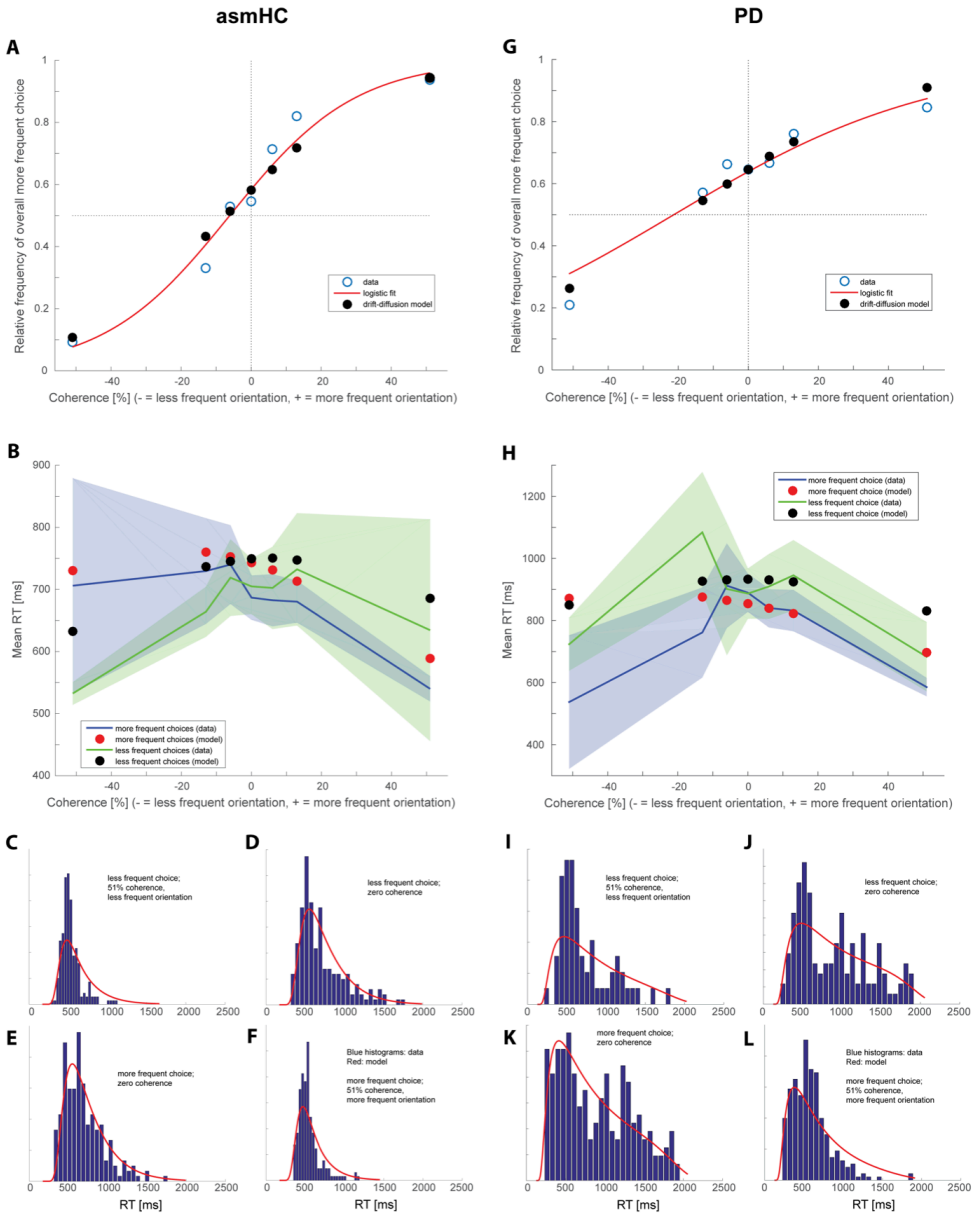

Figure S3. **Model fits for choices and RTs for the monochromatic task. Related to Figure 3.** Otherwise same as in Figure S2 (A-L).

Table S1: Demographic of participants. Related to Figures 1-4

	Age- and sex matched healthy participants	Patients with Parkinson's Disease	p-values
Age			
Dichromatic	62.5 (8.1)	65.75 (9.4)	0.35
Monochromatic	55.8 (6.5)	63.1 (9.7)	<0.05
Explicit	n.a.	62 (8.2)	n.a.
sMMSE			
Dichromatic	29 (1.4)	28 (1.2)	0.48
Monochromatic	29 (1.2)	29 (1.1)	0.73
Explicit	n.a.	29 (1.03)	n.a.
BDI			
Dichromatic	2(2.5)	4(2.5)	<0.01
Monochromatic	2.5 (2.3)	5.5 (4.6)	<0.001
Explicit	n.a.	4(3.3)	n.a.
UPDRS III (no rigidity)	n.a.	13(6.7)	n.a.
Hoehn and Yahr	n.a.	1.5 (0.6)	n.a.
Years since onset	n.a.	4.0 (3.6)	n.a.

Average values and standard deviation between parentheses. sMMSE: Standardized mini Mental State Examination; BDI: Beck Depression Inventory; UPDRS III: Unified Parkinson's Disease Rating Scale, Part III.

Table S2: Model parameters for the dichromatic task. Related to Figure 2

Parameter		Age-sex-matched healthy participants		Patients with Parkinson's disease	
		Parameter value	**SE**	**Parameter value**	**SE**
Proportionality factor between coherence and drift rate k		$0.0135\frac{1}{s\cdot\%coh}$	$0.0002\frac{1}{s\cdot\%coh}$	$0.0131\frac{1}{s\cdot\%coh}$	$0.0002\frac{1}{s\cdot\%coh}$
Diffusion coefficient (variance/time)		$0.477\frac{1}{s}$	$0.004\frac{1}{s}$	$0.468\frac{1}{s}$	$0.003\frac{1}{s}$
Scaling parameter for collapsing bounds s		$2.96\frac{1}{s}$	$0.01\frac{1}{s}$	$2.37\frac{1}{s}$	*
Delay parameter for collapsing bounds d		$255\ ms$	$3\ ms$	$403\ ms$	*
Residual time t_0		$210\ ms$	$1\ ms$	$167\ ms$	$2\ ms$
Stimuli with equal priors: 1st half of trials	Starting point of evidence accumulation	0.064	0.007	–0.036	0.010
	Drift rate offset o	$-0.043\frac{1}{s}$	$0.011\frac{1}{s}$	$0.021\frac{1}{s}$	$0.021\frac{1}{s}$
Stimuli with equal priors: 2nd half of trials	Starting point of evidence accumulation	0.101	0.009	–0.040	0.012
	Drift rate offset o	$-0.141\frac{1}{s}$	$0.020\frac{1}{s}$	$0.041\frac{1}{s}$	$0.020\frac{1}{s}$
Stimuli with unequal priors: 1st half of trials	Starting point of evidence accumulation	0.044	0.007	–0.037	0.011
	Drift rate offset o	$0.077\frac{1}{s}$	$0.010\frac{1}{s}$	$0.074\frac{1}{s}$	$0.021\frac{1}{s}$
Stimuli with unequal priors: 2nd half of trials	Starting point of evidence accumulation	0.081	0.009	–0.050	0.009
	Drift rate offset o	$0.091\frac{1}{s}$	$0.019\frac{1}{s}$	$0.184\frac{1}{s}$	$0.016\frac{1}{s}$

* = likelihood function was too asymmetric for a Gaussian approximation

Table S3: Model parameters for the monochromatic task. Related to Figure 3.

Parameter		Age-sex-matched healthy participants		Patients with Parkinson's disease	
		Parameter value	SE	Parameter value	SE
Proportionality factor between coherence and drift rate k		$0.0185\frac{1}{s\cdot\%coh}$	$0.0003\frac{1}{s\cdot\%coh}$	$0.0183\frac{1}{s\cdot\%coh}$	$0.0004\frac{1}{s\cdot\%coh}$
Diffusion coefficient (variance/time)		$0.365\frac{1}{s}$	$0.002\frac{1}{s}$	$1.02\frac{1}{s}$	$0.01\frac{1}{s}$
Scaling parameter for collapsing bounds s		$5.96\frac{1}{s}$	$0.04\frac{1}{s}$	$2.89\frac{1}{s}$	$0.15\frac{1}{s}$
Delay parameter for collapsing bounds d		$101\,ms$	$2\,ms$	$1.70\,s$	*
Residual time t_0		$161\,ms$	$1\,ms$	$116\,ms$	$3\,ms$
Baseline block	Starting point of evidence accumulation	-0.005	0.008	0.028	0.014
	Drift rate offset o	$0.026\frac{1}{s}$	$0.017\frac{1}{s}$	$-0.141\frac{1}{s}$	$0.031\frac{1}{s}$
1st half of block with unequal priors	Starting point of evidence accumulation	0.025	0.008	0.009	0.015
	Drift rate offset o	$0.107\frac{1}{s}$	$0.020\frac{1}{s}$	$0.184\frac{1}{s}$	$0.025\frac{1}{s}$
2nd half of block with unequal priors	Starting point of evidence accumulation	0.045	0.008	0.048	0.014
	Drift rate offset o	$0.202\frac{1}{s}$	$0.016\frac{1}{s}$	$0.291\frac{1}{s}$	$0.032\frac{1}{s}$
Final block with equal priors	Starting point of evidence accumulation	-0.015	0.009	0.049	0.016
	Drift rate offset o	$0.157\frac{1}{s}$	$0.022\frac{1}{s}$	$0.026\frac{1}{s}$	$0.032\frac{1}{s}$

* = likelihood function was too asymmetric for a Gaussian approximation

Table S4: Model parameters for the explicit task. Related to Figure 4.

Parameter		Patients with Parkinson's disease	
		Parameter value	SE
Proportionality factor between coherence and drift rate k		$0.0118 \frac{1}{s \cdot \%coh}$	$0.0002 \frac{1}{s \cdot \%coh}$
Diffusion coefficient (variance/time)		$0.373 \frac{1}{s}$	$0.004 \frac{1}{s}$
Scaling parameter for collapsing bounds s		$3.51 \frac{1}{s}$	$0.03 \frac{1}{s}$
Delay parameter for collapsing bounds d		$263\ ms$	$6\ ms$
Residual time t_0		$276\ ms$	$2\ ms$
Stimuli with equal priors: 1st half of trials	Starting point of evidence accumulation	-0.003	0.010
	Drift rate offset o	$-0.035 \frac{1}{s}$	$0.019 \frac{1}{s}$
Stimuli with equal priors: 2nd half of trials	Starting point of evidence accumulation	-0.021	0.011
	Drift rate offset o	$0.039 \frac{1}{s}$	$0.020 \frac{1}{s}$
Stimuli with unequal priors: 1st half of trials	Starting point of evidence accumulation	0.000	0.010
	Drift rate offset o	$0.027 \frac{1}{s}$	$0.018 \frac{1}{s}$
Stimuli with unequal priors: 2nd half of trials	Starting point of evidence accumulation	-0.052	0.010
	Drift rate offset o	$0.167 \frac{1}{s}$	$0.019 \frac{1}{s}$

Table S5: Comparison between models that have either only one mechanism for implementing choice bias or two. Related to Figures 2 and 3.

Log likelihoods	Only starting point offsets	Only drift rate offsets	Both types of offsets
Dichromatic asmHC	-63535	-63548	-63512
Dichromatic patients with Parkinson's disease	-45632	**-45608**	**-45604**
Monochromatic asmHC	-46862	-46853	-46830
Monochromatic patients with Parkinson's disease	-46586	**-46567**	**-46559**

The bold numbers indicate a difference in the log likelihood that is too small to justify the addition of a second mechanism according to BIC. asmHC: age- and sex matched healthy participants.

SUPPLEMENTAL EXPERIMENTAL PROCEDURES

This work was reviewed, approved and conducted following the regulations of the Institutional Review Board of the University of California, Los Angeles and only after all participants signed a consent form.

Psychophysics

Participants. We recruited 102 young healthy control participants (yHC), 27 age- and sex- matched healthy control participants (asmHC) and 30 patients with Parkinson's disease with normal or corrected-to-normal vision and without any history of neurological conditions other than Parkinson's disease. Color vision was tested in all participants prior to the experiment using an online version of the Ishihara Color Test. We tested both asmHC and patients using Part III (the motor assessment) of the Unified Parkinson's Disease Rating Scale (UPDRS) excluding rigidity and postural stability. We tested the unilaterality of the motor symptoms and the stage of the disease by means of the UPDRS, the Hoehn and Yahr scale, and the patients' medical history. We use the Mini Mental State Examination (MMSE) to exclude people with dementia and the Beck Depression Inventory (BDI) to exclude people with depression. We excluded people who were unable to discriminate the visual stimulus with accuracy equal to or greater than 90% during practice trials with the easiest discrimination condition (51 and 100% coherence stimuli; 3 yHC, 2 asmHC and 4 patients) and people with a BDI score at or higher than 14 (3 healthy controls). Participants received a compensation of $30.00 for a 2 hour-session and free parking. Students received two class credits for their participation. All patients were under the following medications for Parkinson's disease: levodopa-carbidopa (19/26 patients), dopamine agonists (10/26 patients), inhibitor of monoamine oxidase (13/26 patients). The demographics of our patient and control sample are shown in Table S1.

Visual Stimuli. Leon Glass discovered that if two identical dot patterns are superimposed and one pattern is translated in position with respect to the other, a robust percept of orientation appears (Figure 1B) [S1-S4]. This stimulus, called a Glass pattern, is interesting because at the level of individual dots there is no information about orientation. The brain must integrate the local correlations between the dots (or dot pairs) over the whole display to perceive the orientation. This feature allows us to manipulate parametrically, the difficulty of the task by varying the percentage of the dot pairs that are locally correlated (coherence). In the stimulus with 100% coherence, all the dots are paired so the orientation signal is strong and therefore, the decision is easy. In the 0% coherence pattern there is no orientation signal. These trials are difficult because there is uncertainty about the orientation of the stimulus. In fact, the 0% coherence condition is impossible and we expect choice responses to be pure guesses. By varying dot pair coherence across a range from 0 - 100%, we could vary the difficulty or the orientation discrimination. We used dynamic Glass patterns made with 30 frames of translational patterns sequentially presented at a rate of 85 frames/s. Each frame contained 150 dots, with a size of 0.1° degree and separated by 0.18° degree. For the eye-tracking version of the task, visual stimuli were displayed using custom software (glVex) developed at the National Eye Institute (NEI), running on a dedicated Pentium PC with a video card (NVIDIA Quadro 600) set to provide 8bit grayscale resolution. The code for generating Glass patterns was generously provided by Dr. A. Movshon [S5, S6] .The video PC is a slave device to the PC used for experimental control and data acquisition, REX [S7]. A photocell was placed on the display screen that sends a TTL pulse to the experimental PC providing an accurate measure of stimulus timing. Participants sat at a distance of 57 cm from the monitor and eye movements were tracked with the infrared EyeLink 1000 camera, after appropriate calibration. The luminance of the stimuli using this display was 0.60 cd/m^2 for the green, 0.49 cd/m^2 for the red, 0.63 cd/m^2 for the white patterns. The luminance of the fixation point was 0.38 cd/m2. The background luminance was 0.30 cd/m^2. For the button press version, we used a Macintosh Pro laptop running Psychtoolbox-3 for Apple OS X, under Matlab 64-Bit (Version 8.4.0.) to create and display visual stimuli with an Intel Iris Pro 1024 MB video card on a retina display. The mean luminance was 0.59 cd/m^2 for the green pattern, 0.54 cd/m^2 for the red pattern and 0.60 cd/m^2 for the white pattern. The luminance of the fixation point was 0.28 cd/m^2. The background luminance was 0.19 cd/m2. Since the data for both the button press and the eye movement responses were similar, we pooled the data for this report for all figures except that shown in Figure S1C.

Task design. We developed a novel, two-alternative forced choice task in which participants determined the orientation of Glass pattern visual stimuli with certain or uncertain sensory information. Participants reported their decisions by moving their eyes to one of two cues placed in the visual field corresponding to

the direction of orientation of the Glass pattern or by pressing a button on a keyboard (O = left choice; P = right choice) with one hand. At the beginning of each trial, participants maintained their gaze on a centrally-located fixation point (1000ms ± 200ms determined from an exponential distribution to avoid timing prediction). Then, two choice targets appeared, followed by the onset of the Glass pattern stimulus. Figure S1 shows the validation of this task in healthy control participants. In the three versions of the task (dichromatic, monochromatic, and explicit), participants were informed that they could report their choice as soon as they decided (reaction time (RT) task) but the centrally-located spot remained illuminated in the key press task to encourage continued fixation. In the eye movement version, the fixation point disappeared at the same time that the Glass pattern appeared to indicate that they could report their decision as soon as it was made. We discouraged anticipatory, non-sensory based choices by excluding trials with RTs < 200ms and we excluded trials in which participants failed to respond within 2000ms ± 200ms. This number was determined from the slowest RT of patients (mean ~2100ms). Auditory feedback occurred immediately after every correct response and no feedback occurred for error trials. In the dichromatic and monochromatic tasks we assessed the role of trial to trial feedback in two separate naïve groups of young healthy control participants (yHC), by removing the auditory feedback delivered after every correct trial (see Figure S1E and S1G). We compared this performance to choice performance with auditory feedback (see Figure S1E and S1G). We did not give any explicit reward in any versions of the task.

Dichromatic task. A red Glass pattern and a green Glass pattern appeared on randomly interleaved trials. After the initial block of practice trials with 100% coherence stimuli, we presented 320 green Glass patterns and 320 red Glass patterns with four levels of coherence (100%, 35%, 13%, and 0%), for a total of 640 trials. Whether the red or green pattern appeared was determined randomly but the direction, leftward or rightward, occurred randomly for only one colored stimulus and occurred 75:25 for the other colored stimulus. The direction and the color of the stimulus associated with the unequal priors were counterbalanced across participants. This version of the task has two significant advantages. First, the implicit statistics that participants had to learn are subtle because among all the stimuli that appeared during one session (320 green and 320 red), only 62.5% were oriented in the same direction (compared to 80% in the monochromatic task). Second, this design allowed us to collect equal (one color) and unequal prior (other color) trials at essentially the same time point since the red or green Glass pattern occurrences were randomly interleaved. Therefore, the data collection between unequal and equal prior trial types was not confounded by fatigue or practice effects. Because it takes time to accumulate the priors in this task (see Figure S1E) we only plotted the proportion of positive choices for the second half of the experimental block.

Monochromatic task. After a block of practice trials with 100% coherence stimuli, participants performed three blocks for a total of 800 trials. On each trial, a white on black Glass pattern with four levels of coherence (51%, 13%, 6% and 0%) appeared on the screen on randomly interleaved trials and participants responded by moving their gaze or by pressing a key. During the first block we presented 200 stimuli, half of the stimuli were leftward oriented Glass patterns and half were rightward oriented Glass Patterns. The next block consisted of 400 stimuli unevenly distributed between leftward and rightward Glass patterns (unequal priors): For example, 80% leftward and 20% rightward (80:20) or vice versa. The orientation associated with the higher probability of occurrence was counterbalanced across participants. The last block was the same as the first having an equal number of leftward and rightward Glass patterns (50:50). Participants received short breaks every 200 trials or as requested. In this version of the task, we did not inform participants about the blocks or the presence of the unequal priors. In spite of this, most participants, including patients, reported detecting the difference in the frequency of occurrence of the leftward or rightward stimulus. The timing of the task and the auditory feedback provided were the same as in the dichromatic task. Two of the patients participating in this task also participated in the dichromatic task in two sessions ~8 months apart.

Explicit task. This experiment used all the same methods as used in the dichromatic task except participants received explicit instructions about the task statistics. For example, if the contingences were red, left:right 50:50 and green, left:right 75:25, participants were told that the left direction would occur more often than the right direction for the green stimulus. Six of the patients who participated in the dichromatic task also participated in this task in two sessions ~5 months apart. The yHC participating in the explicit task received only verbal instructions about the priors; there was no implicit trial to trial feedback. This ensured the

validity of the explicit manipulation (see Figure S1H). Patients performing this task in contrast, received both explicit verbal instructions about the priors and trial to trial feedback.

Data analysis. Data were analyzed using a custom GUI based software that allowed the experimenter to mark the occurrence of eye movements and make measurements from analog data. We also used Matlab R2014b for further analysis and construction of plots. Psychometric data were fitted with a logistic function of the form, $p(P) = \lambda + (1-2*\lambda)/(1+\exp(-\beta (C-\alpha)))$; where $p(P)$ is the proportion of positive choices and C is dot pair coherence. α and β are free parameters determined using maximum likelihood methods, and provide a measure of the slope or sensitivity of the psychometric function (β) and the response bias (α). The lapse rate λ is the difference between the asymptote of the function and perfect performance. It is assumed to arise from transient lapses in attention during task performance [S8]. We measured goodness of fit for each participant by calculating the Pearson's residuals for the equal prior condition and performed a chi-square test to ensure that the logistic model fitted the data well. We included participants for which the chi-square test was >0.05, indicating that the expected and observed values are not significantly different and, therefore, indicate good model fits. Figure S1A shows schematic representations of the fits and parameters. We assessed normality of the data using the Kolmogorov-Smirnov with Lilliefors Significance Correction and used parametric tests or non-parametric test as appropriate. In line with the gold standard of psychophysics, we assessed the use of priors by comparing the α values between the equal and the unequal prior condition within groups (paired *t*-test), and we assessed changes in the sensitivity by comparing the β values between equal and unequal prior conditions within groups (paired *t*-test). To compare the use of the priors across groups of participants we measured the proportion of more frequent choices for the most difficult stimulus conditions according to their psychometric functions (0% and 13% for the dichromatic and explicit task; 0% and 6% for the monochromatic task). We then performed a 2X2 mixed ANOVA. The between groups were: patients versus asmHC; or symptomatic versus opposite to symptomatic side; or patients in the dichromatic versus patients in the explicit task. The within-group variable was prior condition: equal and unequal. When appropriate, we performed further post-hoc analyses. To assess the role of trial-to-trial feedback over time and between groups, we first normalized the proportion of more frequent choice to the mean of the first ten trials for the 0% coherence stimuli. We only looked at the 0% coherence stimuli because feedback is most informative when the stimulus is fully ambiguous. To assess rate of prior learning, we computed a linear regression from the first data point to the last data point. To assess the difference in the use of the prior between groups, we used a mixed 2X2 ANOVA with participant group as one factor (with and without feedback) and time (first half and second half) as the second factor. We used Kruskal Wallis tests when normality test failed. Analyses were run using IBM SPSS Statistics for Macintosh, Version 23 and/or Matlab R2014b.

Drift Diffusion Model. We used the drift-diffusion model (DDM) framework to model choices and reaction time (RT) distributions. Upon inspection of the data, we found that some of the RT distributions did not exhibit the long exponential tails that would be expected from a standard drift-diffusion model (see, e.g., Figure S2C-F). In addition, we found asymmetry in mean RT between error responses (longer) and correct responses (shorter). This can be seen, for example, in Figure S3B. Green choices are correct in the left half of the plot, whereas blue choices are correct in the right half of the plot. Their mean RTs are shorter than those of the opposite choice (other color errors). These properties of RT distributions suggest that, as time passes, the decision process terminates with a smaller amount of accumulated evidence [S9]. This phenomenon is also known as an "urgency" mechanism and can be implemented in different ways (collapsing decision bounds, time-variant gain, etc.) with very similar predictions for decision behavior. Here, we use collapsing decision bounds. The models were fitted to the pooled data across participants. Five model parameters were kept fixed across task epochs and across stimulus colors in the dichromatic task: proportionality factor between coherence and drift rate, the diffusion coefficient, the collapsing bound scaling parameter, the collapsing bound delay parameter, and the residual time. In the dichromatic task, we estimated four different pairs of starting point of evidence accumulation and drift rate offset, for the four possible combinations of the two stimulus colors and two experimental epochs (first half and second half of the trials). In the monochromatic task we also estimated four different pairs of starting point and drift rate offset for the four different experimental epochs (first equal prior block, first half of the unequal prior block, second half of the unequal prior block, second equal prior block). The estimated model parameters can be found in Table S2 for the dichromatic task, in Table S3 for the monochromatic task, and in Table S4 for the explicit task.

We used a chi-square variance test to assess whether the variance of starting points of evidence accumulation across experimental conditions exceeded the expected variance if the starting point did not change, which is determined by the standard errors of the parameter estimates. Thus, we tested whether the null hypothesis that the starting points did not change across experimental conditions had to be rejected based on the estimated starting points. Since we always estimated four different starting points (SP), the test statistic was

$$\chi^2 = \frac{3 \cdot \sigma^2_{SP\ across\ conditions}}{0.25 \cdot \sum_{i=1}^{4} \sigma_i^2}$$

with three degrees of freedom. The denominator is the average of the squared standard errors of the estimated parameters, i.e., the expected variance if the starting point did not change across conditions.

Model structure and parameter estimation

Evidence accumulation begins at a starting point that is determined by one of the model parameters and continues until one of two decision thresholds is crossed. The upper bound is located at

$$B_{upper}(t) = \frac{1}{1+\exp\left(s \cdot \left(t-d\right)\right)} + \frac{\exp\left(-s \cdot d\right)}{1+\exp\left(-s \cdot d\right)}$$

the lower bound at

$$B_{lower}(t) = -B_{upper}(t)$$

The bounds start at ± 1 for $t = 0$ and then start collapsing. The scaling parameter s determines how quickly the bounds collapse, the delay parameter d determines when the bounds start collapsing. The boundary functions are identical to the ones used in S9]. The drift rate r is given by

$$r = k \cdot C + o$$

with $|C|$ being the coherence of the stimulus. The sign of C is chosen such that it is positive when the stimulus orientation is the one that ocurred more frequently in the unequal prior situation and negative for the opposite orientation. o represents a drift rate offset, which is one of two mechanisms, in addition to adjusting the starting point of evidence accumulation, that can be used to implement a decision bias. The diffusion coefficient was assumed to be fixed (independent of stimulus strength). The first threshold crossing terminates the decision and determines choice and decision time. Crossing the upper bound first would trigger the choice that should be more frequent in the unequal prior situation. RT is obtained by adding a constant residual time t_0 to the decision time:

$$RT = t_{decision} + t_0$$

Model predictions (probabilities of each choice and RT distributions for each coherence level and stimulus orientation) were obtained by solving a pair of integral equations numerically [S10]. Details regarding the implementation can be found in [S9], Appendix B, Model 1: Evaluation of the model performance. The method is implemented in the Stochastic Integration Modeling Toolbox for MATLAB, developed by J. Ditterich, which can be downloaded from http://master.peractionlab.org/software.

The optimal set of parameters was obtained using maximum likelihood estimation, combining a multidimensional simplex approach ("fminsearch" in the MATLAB Optimization Toolbox) with a pattern search algorithm ("patternsearch" in the MATLAB Global Optimization Toolbox) to avoid getting stuck in local optima. Standard errors of estimated model parameters were obtained using a 1-dimensional local Gaussian approximation of the likelihood function L around the optimal value p_{opt} of a particular parameter p:

$$L(p) \approx L_{\max} \cdot \exp\left(-\frac{\left(p-p_{opt}\right)^2}{2 \cdot \sigma_p^2}\right)$$

with σ_p being the standard error of the parameter estimate.

The models were fitted to the pooled data across participants. In the dichromatic task, we excluded two patients from the modeling dataset, one because the data were collected using a different set of coherence levels than all the other participants and one because the RTs were substantially slower than those of all the other patients, which would have introduced bimodal RT distributions. This left 11 patients and 12 age- and sex-matched controls (asmHC). In the monochromatic task, we used the 8 asmHC and the 9 patients with Parkinson's disease for which we had experimental data from all epochs. In the case of the explicit task, model parameters were also estimated from the pooled data of 9 patients.

Five model parameters were required to remain the same across task epochs and across stimulus color in the dichromatic task: proportionality factor k between coherence and drift rate, diffusion coefficient, collapsing bound scaling parameter s, collapsing bound delay parameter d, and the residual time t_0. Four different pairs of starting points of evidence accumulation and drift rate offsets o were estimated for each of the datasets: for two different time windows and each stimulus color in the dichromatic task and for four different time windows in the monochromatic task. The estimated model parameters can be found in Table S2 for the dichromatic task, in Table S3 for the monochromatic task, and in Table S4 for the explicit task (patients only). Since we cannot show the correspondence between data and model predictions for all 16 task epochs, we show four representative examples, one for each dataset, in Figures S2 and S3. Our goal was not to develop a complex model that could account for all details of the data, but to use the simplest possible model that could capture the main features of the data. Since 8 model parameters were needed to implement the two bias mechanisms, the number of remaining model parameters was kept as small as possible.

To further assess how important the presence of two different mechanisms for implementing bias was for being able to explain the data we also fitted models that had only one of the two mechanisms: either only starting point offsets or only drift rate offsets. The resulting log likelihoods are shown in Table S5. A larger log likelihood value (smaller negative number) indicates a better fit. Adding the second mechanism almost always led to a clear improvement in the model's ability to account for the data with only two exceptions: For the patients (dichromatic and monochromatic task), when starting with a model that only had drift rate offsets, adding the starting point offsets did not improve the likelihood enough to justify the increase in the number of model parameters according to the Bayesian Information Criterion (BIC). This is indicated with the bold numbers in Table S5. The minimum improvement in the log likelihood to justify the addition of the second mechanism would be

$$\frac{\#\ of\ additional\ parameters \cdot \ln\left(\#\ of\ trials\right)}{2}$$

Since we had on the order of 6,500 trials per dataset, this is ~18. Our findings indicate that healthy control participants took advantage of both mechanisms for implementing bias and provide further evidence for patients with Parkinson's disease being impaired in the use of starting point offsets for exploiting prior information.

Is there evidence for lower decision thresholds in patients with Parkinson's disease?

In the main paper we addressed whether patients with Parkinson's disease could make asymmetric adjustments to their decision thresholds based on prior information, i.e., whether they could decrease the amount of evidence needed for one choice option while increasing the amount of evidence needed for the alternative option. We found that patients with Parkinson's disease were impaired at making these adjustments. However, such an asymmetric adjustment does not affect the distance between the two decision bounds. Thus, we analyzed the difference between the decision thresholds for both options, but not how far away they were from the starting point of evidence accumulation overall. A recent modeling effort suggests that patients with Parkinson's disease should have overall lower decision thresholds when making perceptual choices independent of prior manipulations and when off medication [S11]. Here we sought to test if a lower decision threshold also applied to our patients on medications. When parameterizing a drift-diffusion model there is always one model parameter that can be fixed arbitrarily. Since the decision

bounds always started at ± 1 in our model, a lower decision threshold would show up as a combined change of the proportionality factor k and the diffusion coefficient in our parameter estimates. Choice accuracy in the DDM is determined by $\frac{r \cdot B}{\sigma^2}$ (with r being drift rate, B being height of the decision bound, and σ^2 being the diffusion coefficient) and the mean RT is determined by $\frac{B}{r}$ multiplied by another term that again depends on $\frac{r \cdot B}{\sigma^2}$ [S12]. Therefore, parameter changes that modify both terms in the same way as a change in bound height would be considered equivalent. Reducing bound height by a factor f would result in both terms being divided by f, which could also be achieved by multiplying r with f and by multiplying σ^2 with f^2. In our parameter estimates, a lower decision threshold should therefore appear as an increase in both the proportionality factor between coherence and drift rate k and the diffusion coefficient.

The parameter estimates for the monochromatic task show that although patients with Parkinson's disease had an increased diffusion coefficient (1.02 vs. 0.365; $p < 10^{-6}$, *t*-test), k was not significantly different (0.0183 vs. 0.0185; p=1.00, *t*-test; cf., Table S3). Thus, the parameter estimates are inconsistent with a lower average decision threshold. Rather, the model parameters for the monochromatic task point to a lower signal-to-noise ratio of the sensory evidence signal. Consistent with a lower signal-to-noise ratio, the β parameter of the logistic fit to the choice data for the equal prior condition was 0.008 for patients and 0.012 for asmHC. However, these differences failed to reach statistical significance ($t(18)$=-.55, p>0.05). In the dichromatic task, the estimates of k (0.0131 vs. 0.0135; $p = 0.16$, *t*-test) and the diffusion coefficient (0.468 vs. 0.477; $p = 0.07$, *t*-test) were similar across groups (cf., Table S2).

Therefore, our data do not support the idea that patients have overall lower decision thresholds than asmHC participants, as suggested by the model from Wang and colleagues. This difference in our findings could be explained by the fact that our patients were on medication, so a conclusive answer would require testing in patients off medication.

Finally, we found reliably shorter estimates of the residual time (116 vs. 161 ms in the monochromatic task ($p < 10^{-6}$, *t*-test); 167 vs. 210 ms in the dichromatic task ($p < 10^{-6}$, *t*-test)) in patients. This parameter captures the non-decision components of RT such as the initial sensory processing and the initiation of the movement response. Indeed, this is consistent with the known shorter movement latencies in patients with Parkinson's disease performing visually-guided tasks [S13, S14] and in monkeys with manipulation of basal ganglia processing [S15]. It may also be a sign of impulsivity of action [S16, S17] .

REFERENCES

S1. Wilson, H.R., and Wilkinson, F. (1998). Detection of global structure in Glass patterns: implications for form vision. Vision Research *38*, 2933-2947.

S2. Wilson, H.R., Wilkinson, F., and Asaad, W. (1997). Concentric orientation summation in human form vision. Vision Research *37*, 2325-2330.

S3. Aspell, J.E., Wattam-Bell, J., and Braddick, O. (2006). Interaction of spatial and temporal integration in global form processing. Vision Research *46*, 2834-2841.

S4. Glass, L. (1969). The Moire effect from random dots. Nature *223*, 578-580.

S5. Smith, M.A., Kohn, A., and Movshon, J.A. (2007). Glass pattern responses in macaque V2 neurons. Journal of Vision *7*.

S6. Smith, M.A., Bair, W., and Movshon, J.A. (2002). Signals in Macaque Striate Cortical Neurons that Support the Perception of Glass Patterns. The Journal of Neuroscience *22*, 8334-8345.

S7. Hays, A.V., Richmond, B.J., and Optican, L.M. (1982). A UNIX-based multiple process system for real-time data acquisition and control. WESCON Conf. Proc. *2*, 1-10.

S8. Gold, J.I., and Ding, L. (2013). How mechanisms of perceptual decision-making affect the psychometric function. Progress in Neurobiology *103*, 98-114.

S9. Ditterich, J. (2006). Stochastic models of decisions about motion direction: Behavior and physiology. Neural Networks *19*, 981.

S10. Smith, P.L. (2000). Stochastic Dynamic Models of Response Time and Accuracy: A Foundational Primer. Journal of Mathematical Psychology *44*, 408.

S11. Wei, W., Rubin, J.E., and Wang, X.-J. (2015). Role of the Indirect Pathway of the Basal Ganglia in Perceptual Decision Making. The Journal of Neuroscience *35*, 4052-4064.

S12. Palmer, J., Huk, A.C., and Shadlen, M.N. (2005). The effect of stimulus strength on the speed and accuracy of a perceptual decision. Journal of Vision *5*, 376-404.

S13. Briand, K.A., Strallow, D., Hening, W., Poizner, H., and Sereno, A.B. (1999). Control of voluntary and reflexive saccades in Parkinson's disease. Experimental Brain Research *129*, 38-48.

S14. Briand, K.A., Hening, W., Poizner, H., and Sereno, A.B. (2001). Automatic orienting of visuospatial attention in Parkinson's disease. Neuropsychologia *39*, 1240.

S15. Basso, M.A., and Liu, P. (2007). Context-dependent effects of substantia nigra stimulation on eye movements. J Neurophysiol *97*, 4129-4142.

S16. Amador, S.C., Hood, A.J., Schiess, M.C., Izor, R., and Sereno, A.B. (2006). Dissociating cognitive deficits involved in voluntary eye movement dysfunctions in Parkinson's disease patients. Neuropsychologia *44*, 1475-1482.

S17. Zhang, J., Rittman, T., Nombela, C., Fois, A., Coyle-Gilchrist, I., Barker, R.A., Hughes, L.E., and Rowe, J.B. (2015). Different decision deficits impair response inhibition in progressive supranuclear palsy and Parkinson’s disease. Brain.